Micromechanical Properties and Ductile Behavior of Electrospun Polystyrene Nanofibers

A. Sh. Asran,[1,2] V. Seydewitz,[1] G. H. Michler[1]

[1]*Institute of Physics, Martin-Luther-University Halle-Wittenberg, D-06099 Halle/S., Germany*
[2]*National Research Centre, 12311 Cairo, Egypt*

Received 27 May 2010; accepted 12 April 2011
DOI 10.1002/app.34847
Published online 17 January 2012 in Wiley Online Library (wileyonlinelibrary.com).

ABSTRACT: Using electrospinning technique polystyrene (PS) nanofibers in the thickness range from 150 to 800 nm have been produced. Electron microscope inspections reveal the relatively uniform thickness of the obtained fibers. The mechanical deformation mechanisms have been studied in tension tests using micro-tensile devices for a scanning electron microscope (SEM) and a transmission electron microscope (TEM). A characteristic change in the deformation behavior from the typical craze formation of PS to a micro necking and cold drawing has been found with decreasing fiber thickness. There is a surprisingly sharp fiber thickness limit between both deformation types in the range of 220–225 nm: nanofibers thicker than ~ 225 nm deform with formation of crazes, nanofibers thinner than ~ 225 nm show necking and cold drawing.
 J Appl Polym Sci 125: 1663–1673, 2012

Key words: polystyrene; electrospinning; electron microscopy; micromechanical deformation; craze; necking

INTRODUCTION

Electrospinning is a novel process for forming ultrafine fibers with diameters ranging from 10 μm to 5 nm. It is currently the most widely used method for the production of polymeric nanofibers because of its simplicity, cost-effective, and suitability to yield very long fibers from various polymers and composite materials. The process can be simply carried out by applying a high voltage (several thousand volts/cm) to a capillary filled with polymer fluid (solution or melt), which is ejected out toward a counter electrode serving as the collector. The As spun fibers have received attention due to their unique properties such as low density, large surface area to mass, and high pore volume with controllable pore size.[1,2] Furthermore, it has been demonstrated that the electrospun nanofibers have a good macromolecular orientation along the fibers direction, which is produced by stretching of the polymer jet during electrospinning.[3] The high molecular orientation of polymer molecules in the electrospun nanofibers enhances their mechanical properties (e.g., higher elastic modulus and strength) as compared to bulk materials. Therefore, the combination of high specific surface area, flexibility, and superior mechanical properties makes the nanofibers important material for many applications such as filtration, protective clothing and composite materials, high performance batteries, tissue engineering, and drug delivery.[4–7]

Polystyrene (PS) is a thermoplastic amorphous, stiff polymer with limited flexibility. It is considered to be one of the most versatile, easily fabricated, and cost-effective plastics.[8] It is used in many different applications including packaging for food, disposable cutlery, plastic models, packing materials, insulation, and disposable beverage cups.[9] Recently, PS nanofibers and their nanocomposites have been fabricated by electrospinning technique for different applications.[10–12] The principal disadvantage of PS is its brittleness; in tension the strain at break is only few percentages. However, PS macromolecules can be deformed to a very high degree if they are arranged in very thin fibers or films. This effect is well known from the fibril inside crazes, the typical deformation zones in PS. Crazes are long deformation zones in perpendicular direction to the loading direction, up to some 100 μm long and about 10 μm thick. They posses an internal structure of nanovoids with plastically stretched fibrils about 10–30 nm thick. The fibrils are stretched up to more than 300%,[13] the limit of deformation of the entanglement network.[14]

Measurements of mechanical properties of the as spun nanofibers are very important for understanding their mechanical performance, stability, etc. It is expected to differ from bulk materials because of their large surface area to volume ratio. However, determining the mechanical properties of nanofibers is a difficult task, mainly because of their very small

Correspondence to: G. H. Michler (goerg.michler@physik.uni-halle.de).

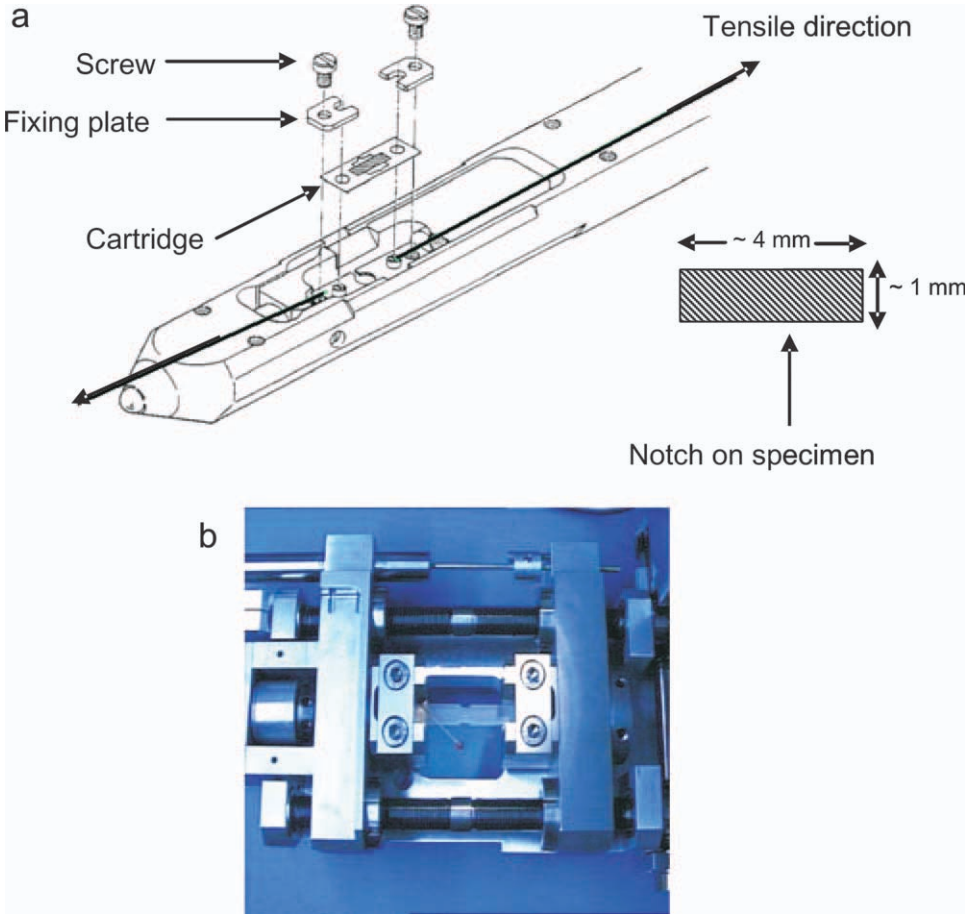

Figure 1 *In situ* deformation devices. (a) Scheme of the miniaturized straining holder from Gatan for a TEM (JEOL, JEM 4010, 400 kV). (b) Straining holder for environmental scanning electron microscopy (ESEM). [Color figure can be viewed in the online issue, which is available at wileyonlinelibrary.com.]

dimensions. Recently, many attempts have been gained to study the mechanical behavior of the nanofibers using different methods.[15] Carlisle et al. determined the mechanical properties of fibrinogen nanofibers using *in situ* imaging method to study their micromechanical deformation and relating the deformation observed to the stress–strain characteristics of the nanofibers.[16] Furthermore, the transition from crazing to shear deformation in polymers and blend polymers has been explored by many authors.[17,18] However, no information exists about the transition from craze to shear of the electrospun

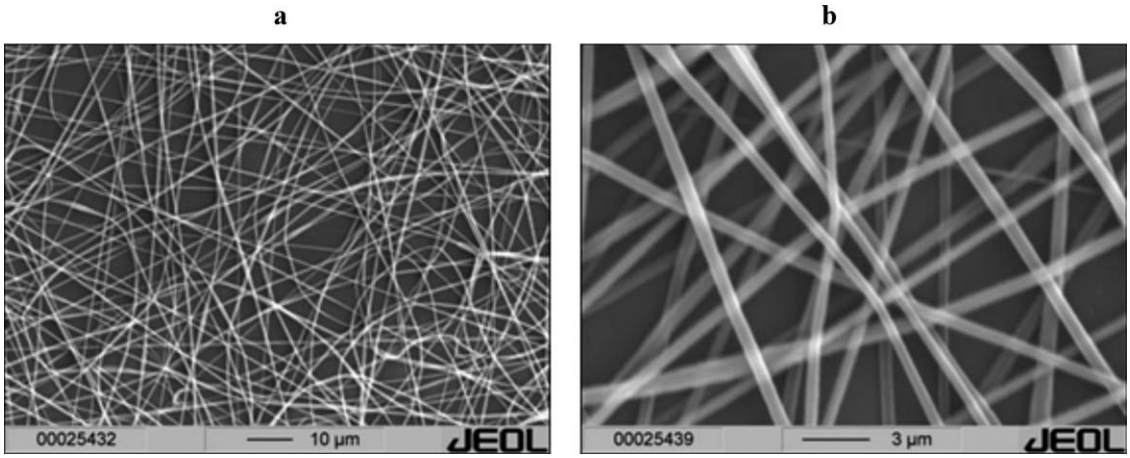

Figure 2 SEM micrographs of PS nanofibers (a,b) in lower and larger magnification.

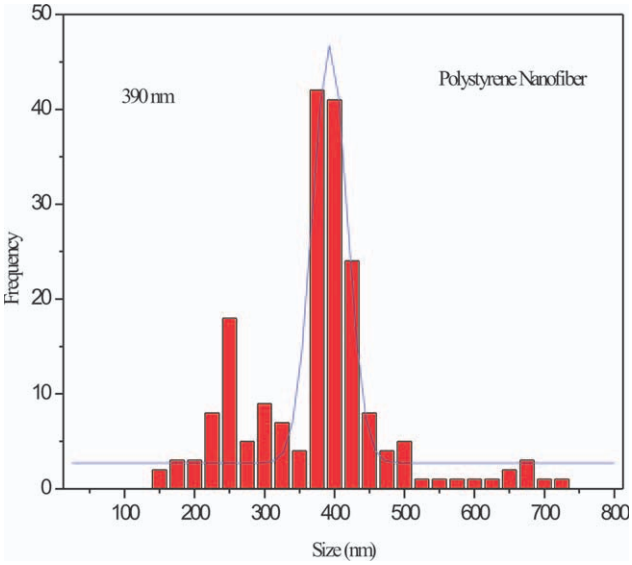

Figure 3 Diameter distributions of PS nanofibers. [Color figure can be viewed in the online issue, which is available at wileyonlinelibrary.com.]

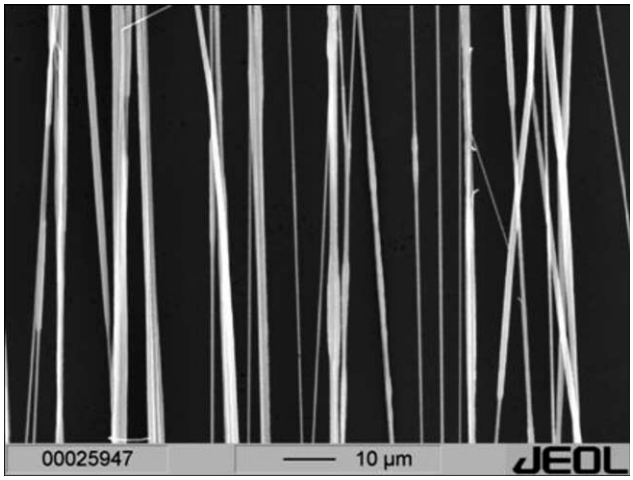

Figure 4 SEM micrograph of uniaxially aligned PS nanofibers.

PS nanofibers. Herein, the aim of this study was to check whether PS nanofibers reveal a transition from the typical crazing behavior of bulk PS to ductile behavior with decreasing the fiber thickness.

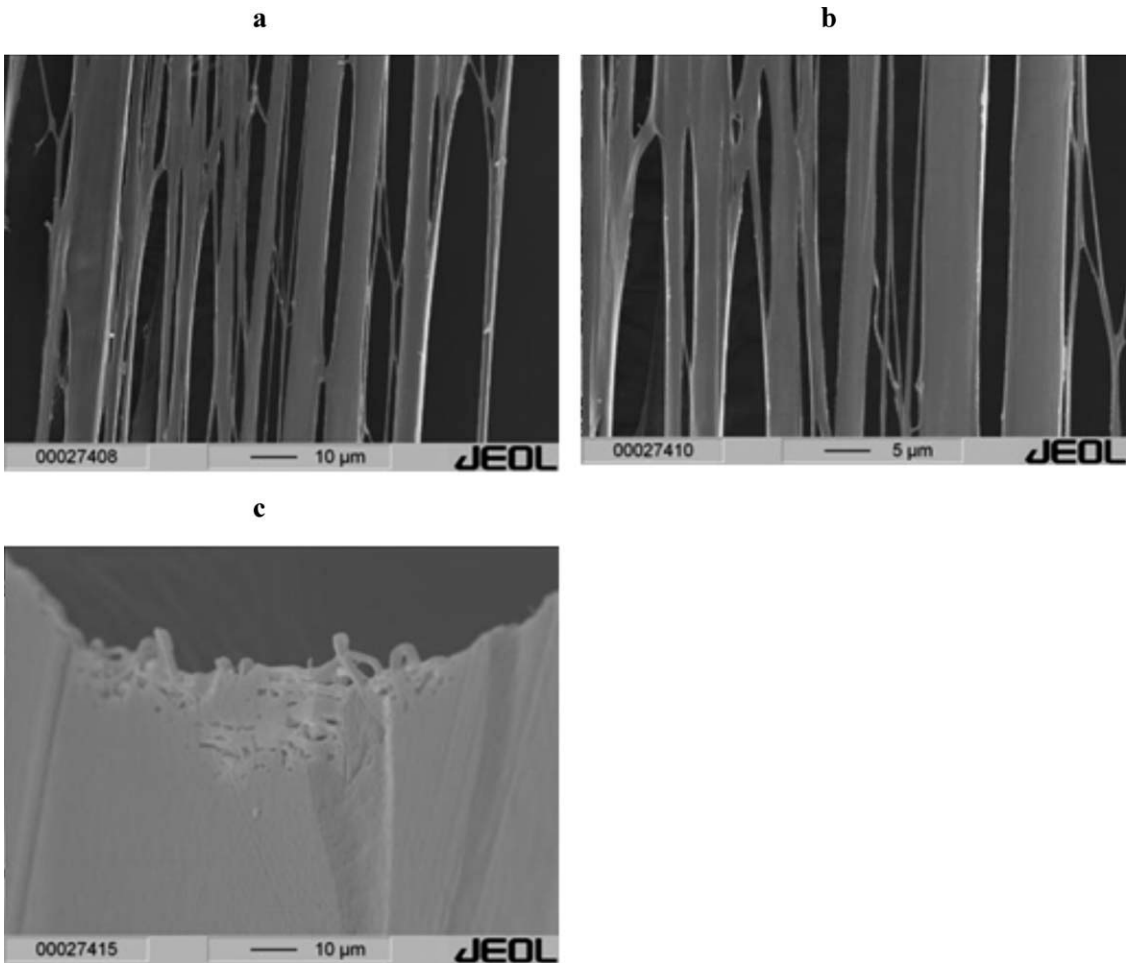

Figure 5 Morphology of a pattern of hot compacted PS nanofibers. (a) Compacted at 85°C with a pressure of 20 MPa for 5 min. (b) Compacted at 85°C with a pressure of 30 MPa for 5 min. (c) Compacted at 90°C with a pressure of 30 MPa for 5 min.

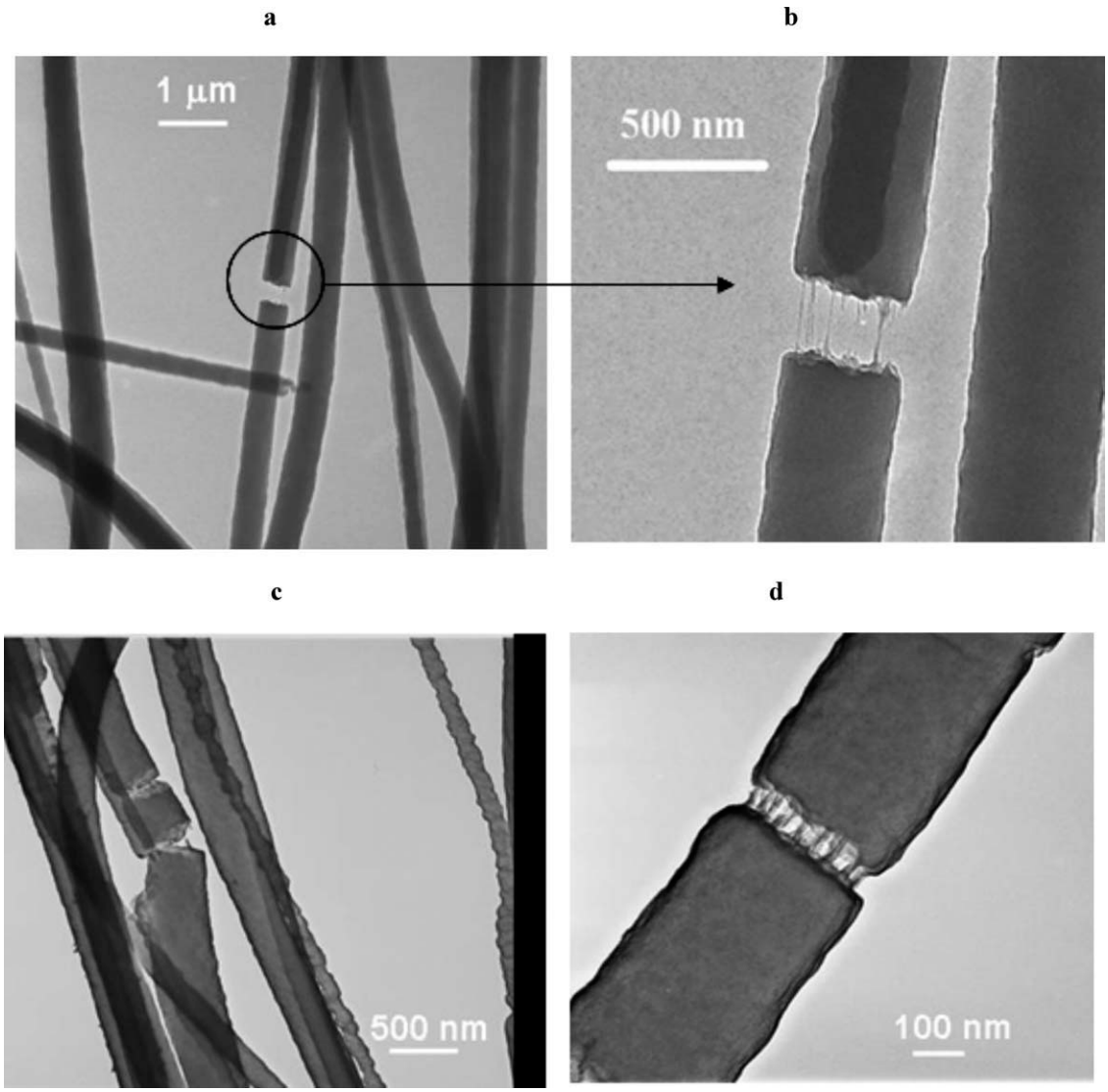

Figure 6 TEM micrographs of deformed PS nanofibers with fibrillated crazes.

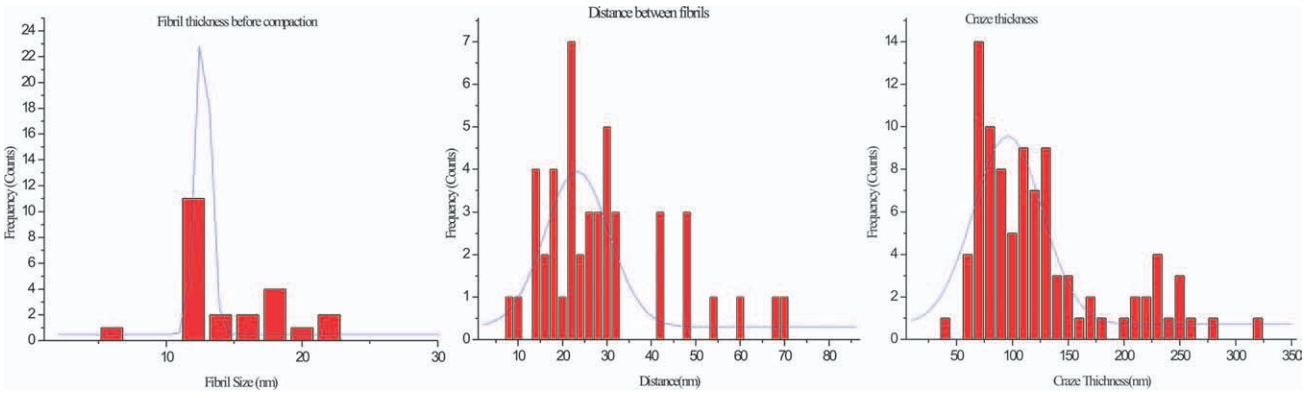

Figure 7 Distribution of craze thickness, craze fibril diameters, and interfibriller distance (long period) in deformed PS nanofibers. [Color figure can be viewed in the online issue, which is available at wileyonlinelibrary.com.]

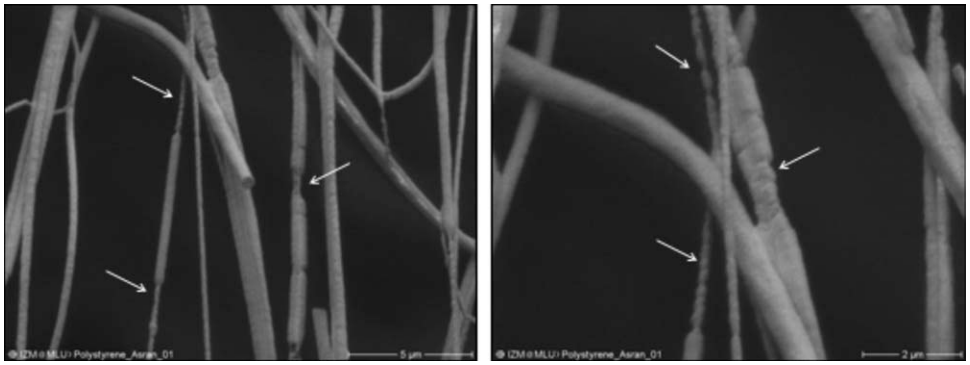

Figure 8 Deformed PS nanofibers ESEM micrographs: local necking zones are shown by arrows.

EXPERIMENTAL

Materials

PS, average molecular weight 120 kDa, was purchased from BASF and used without further treatment or purification. Tetrahydrofurane (THF), and *N*,*N*-dimethylformamide (DMF) to dissolve PS were purchased from Sigma Aldrich, Germany.

Method

Electrospinning process of the PS nanofibers

To obtain electrospinnable solutions, 20 wt% PS was dissolved in (75/25 wt/wt) THF/DMF, and vigorously stirred with a magnetic stir bar at room temperature for 8 h to ensure homogeneity. The polymer solution was filled in a 1-mL syringe attached with a blunt steel needle of 0.8 mm inner diameter. A round steel plate covered with aluminum foil was placed 15 cm away from the needle tip as counter electrode. Electrospinning was carried out at room temperature in a vertical spinning configuration, using the applied voltages 20 kV, driven by a high voltage power supply (Heizinger PNC, Germany) with a flow rate of 1 mL/h. The electrospun fibers were collected directly on an aluminium foil or a glass plate which was placed over the counter electrode as collecting substrate. To study the mechanical deformation behavior, uniaxially aligned PS nanofibers have been prepared by the parallel electrodes method.[19,20]

Hot compaction of aligned PS nanofibers

Multilayer aligned nanofibers membranes were prepared and compacted at different temperatures using a hot compaction technique (Labo press 200 T hot compaction). The hot compaction process applied to the aligned nanofibers mats at a temperature that is below the glass transition temperature of PS (T_g about 105°C). Compactions were at two different temperatures (85°C and 90°C) with a pressure of 20 MPa for 5 min.

Morphological characterization

Morphological studies of the electrospun and hot compacted nanofibers were conducted by electron microscopy. For scanning electron microscope (SEM, JSM 6300 JEOL) inspection, the samples were prepared by direct electrospinning of PS on the slide

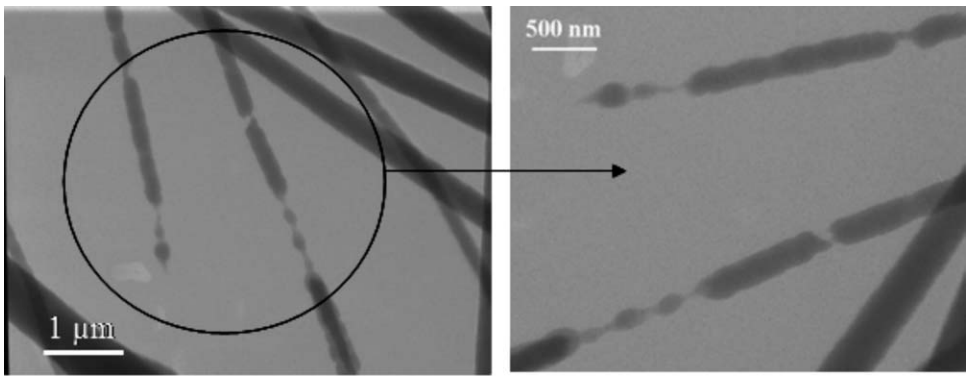

Figure 9 TEM micrographs of deformed PS nanofibers with necking and cold drawing zones in lower (left) and larger magnification (right).

TABLE I
Results of Image Analysis of Deformed PS Nanofibers with Appearance of Crazes or Necking Zones, Respectively

No.	Fiber diameter (nm)	Craze thickness (nm)	Craze fibril diameter (nm)	Observation
1	391	223	8	Crazing No necking
2	614	93	25	Crazing No necking
3	364	57	18	Crazing No necking
4	363	58	12	Crazing No necking
5	378	56	13	Crazing No necking
6	237	112	23	Crazing No necking
7	226	90	17	Crazing No necking
8	264	99	23	Crazing No necking
No.	Fiber diameter (nm)	Length of necking zone (nm)	Neck width (nm)	Observation
9	220	123	52	Necking
10	218	155	52	Necking
11	198	168	65	Necking
12	165	109	88	Necking
13	155	189	57	Necking

glasses and followed by Au sputtering of a 20-nm thick layer for better conductivity during imaging. Average diameters of the electrospun fibers and their size distribution were determined by measuring over 200 fibers selected randomly from the SEM images using image analysis software (Analysis, Soft Imaging System Co., Germany). The morphology of aligned PS nanofibers has been investigated by transmission electron microscopy (TEM, JEOL JEM 4010, 400 kV).

In situ deformation of the PS nanofibers

To study the mechanical deformation structures of the electrospun PS nanofibers, aligned nanofibers were prepared in a miniaturized straining holder from Gatan for a TEM (JEOL, JEM 4010, 400 kV). Straining device, shape, and size of the specimen used in this study are shown in Figure 1.

Differential scanning calorimetry

Differential scanning calorimetry (DSC) measurements were conducted to measure the glass transition temperature (T_g) of the bulk material, nanofibers, and hot compacted PS nanofibers using a Mettler-Toledo DSC 820 under a nitrogen atmosphere. The samples were sealed in aluminum pans and heated and cooled in the temperature range

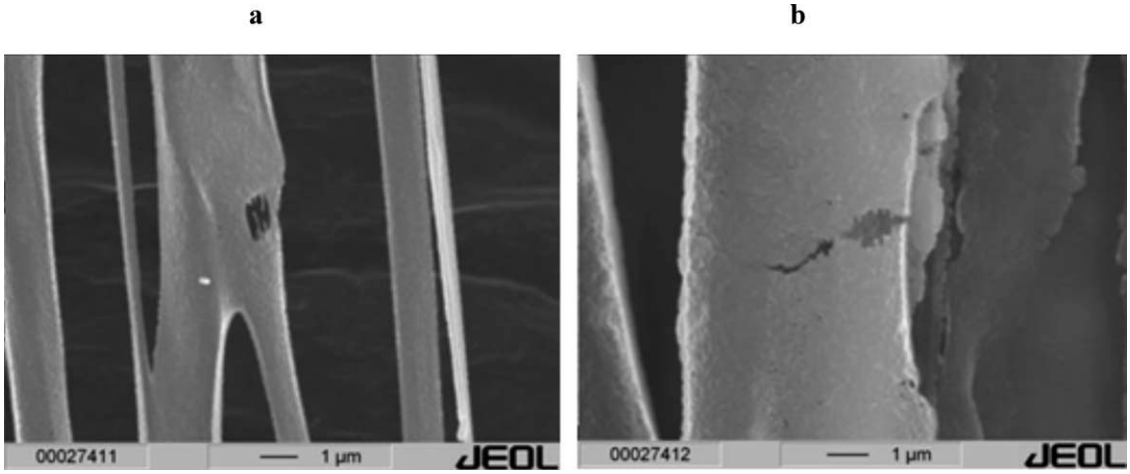

Figure 10 Deformation of hot compacted aligned PS nanofibers: compacted at 85°C with a pressure of 30 MPa for 5 min.

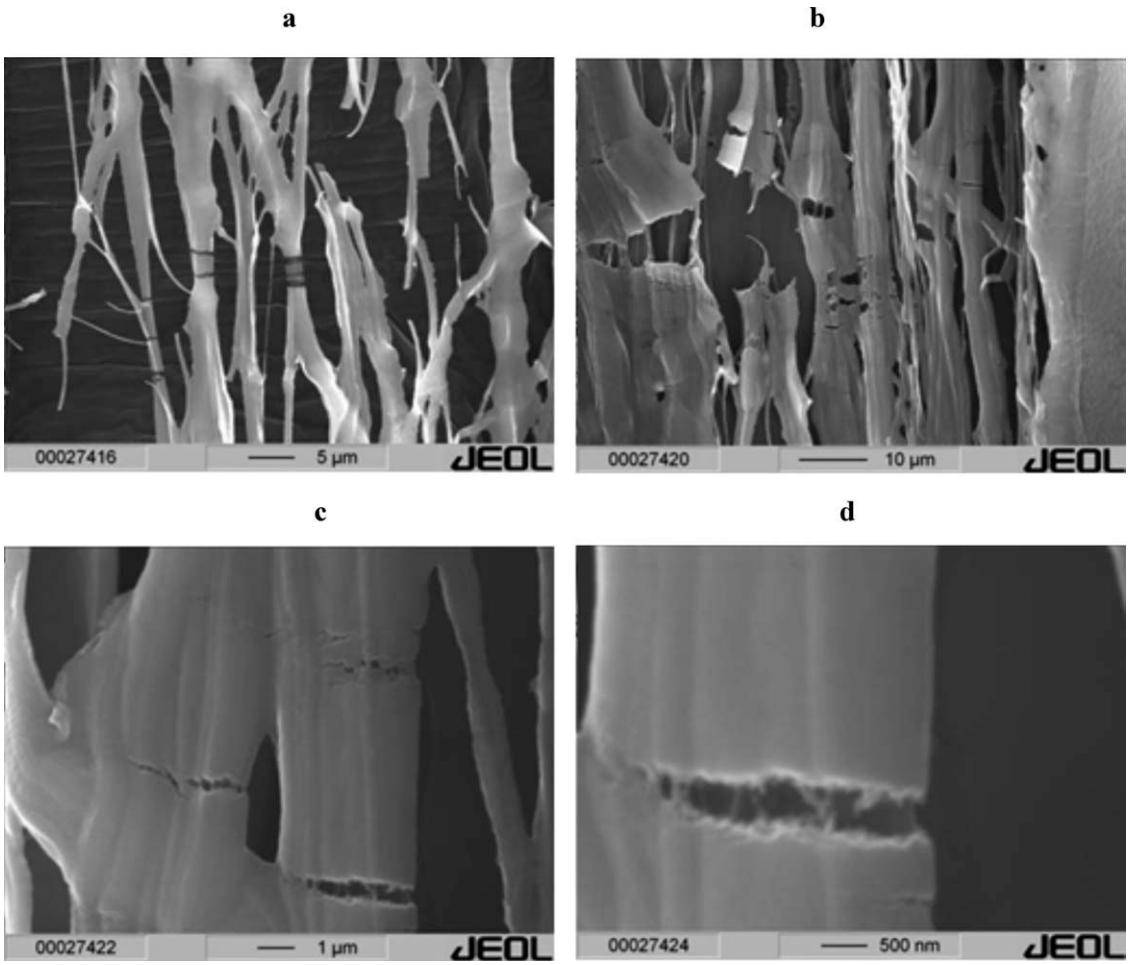

Figure 11 Deformation of hot compacted aligned PS nanofibers: compacted at 85°C with a pressure of 20 MPa for 5 min.

25–150°C in the DSC instrument with a rate of 10 °C/min. The weight of each sample was approximately 0.5 mg. The DSC temperature and heat flow values were calibrated with indium as the standard.

RESULTS

Morphology

Figure 2(a,b) shows SEM micrographs of electrospun PS nanofibers with random orientation. It is visible

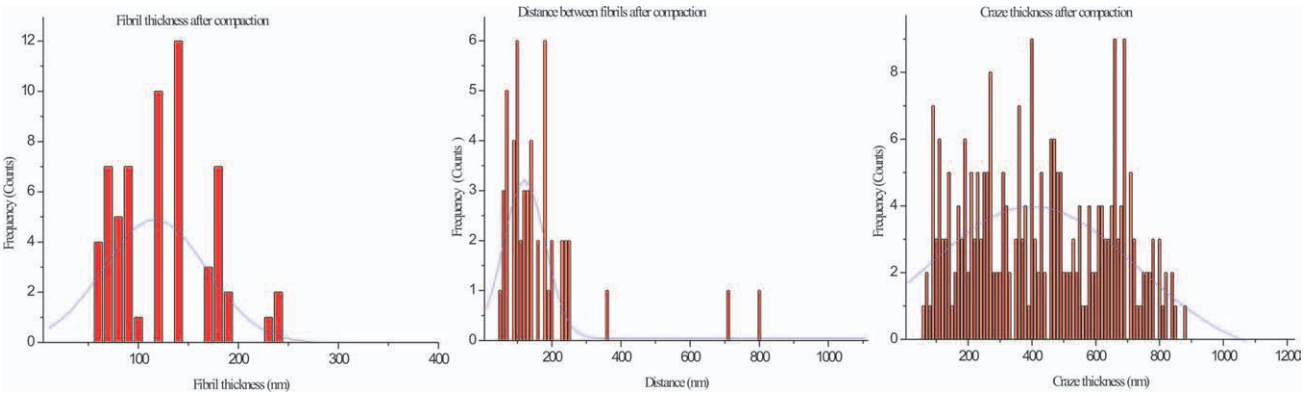

Figure 12 Distribution of craze thickness, craze fibril diameter and interfibrillar distance of deformed hot compacted PS nanofibers (hot compacted at 85°C, 30 MPa). [Color figure can be viewed in the online issue, which is available at wileyonlinelibrary.com.]

TABLE II
Glass Transition Temperatures for Bulk PS, PS Nanofibers, and Hot Compacted PS

Sample no.	Sample description	T_g
Polystyrene I	Granules	105
Polystyrene II	Nanofibers	101
Polystyrene III	Compacted nanofibers at 85°C, 30 MPa for 5 min	99
Polystyrene IV	Compacted nanofibers at 90°C, 30 MPa for 5 min	98

that the individual PS nanofibers are relatively uniform in thickness without any sign of bead formation. The diameters of the electrospun PS nanofiber vary from 150 nm to 800 nm (see Figure 3) and their distribution shows a maximum at ~ 390 nm. Figure 4 shows a SEM micrograph of PS nanofibers uniaxially aligned in one direction. Such patterns of parallel nanofibers have been used to perform tensile tests and also to produce hot compacted specimen. Result of the hot compaction is a compacted pattern of fibers with many free spaces or holes between them, see Figure 5.

Figure 5(a) shows uniaxially aligned PS nanofibers compacted at 85°C with a pressure of 20 MPa for 5 min and Figure 5(b) shows compacted at 85°C with 30 MPa for 5 min. The best temperature for compaction is ~ 85°C with a pressure of 20 MPa and 30 MPa. Many of the original nanofibers are connected to thick fiber bundles up to some μm thickness, but there are visible also thin individual nanofibers. In case of compaction at 90°C (which is near to T_g of PS), the nanofibers adhere together and form a membrane without any sign of fibril structure [Figure 5(c)].

Deformation of electrospun PS nanofibers

Deformation structure of single electrospun PS nanofibers

Figure 6 shows the deformation structures of PS nanofibers mechanically deformed *in situ* in a TEM. There are some places with the appearance of typical crazes before breaking. The craze thickness (elongation of crazes in direction of fibril length) is about 120 nm, the craze fibrils are ~ 20 nm thick and the interfibrillar spacing between craze fibrils (long period) is about 25 nm (Figure 7). Appearance of crazes in similar structure has been detected in all PS fibers with diameters above 225 nm.

Figure 8 shows ESEM micrographs of deformed and partially ruptured PS nanofibers. It is an interesting result that some fibers show thinner parts due to necking and cold drawing. The same effect is visible after deformation in the TEM (see Figure 9).

A detailed inspection revealed that fibers with necking and cold drawing are all thinner than 225 nm, see Table I. The fiber diameter contracted from ~ 225 nm to nearly 60 nm in the neck regions. The length of the neck zone is in the range from 100 nm to 200 nm and partly some necking zones follows one after the other. Partly there are thin cold drawing zones with a total length of these zones of some micrometers.

It is a surprising result that the transition in the micromechanical behavior appears at thicknesses of the PS fibers between 220 and 225 nm, i.e., at a sharp limit PS fibers thicker than this limit show only craze deformation and PS fibers thinner than that reveal only necking and cold drawing.

Deformation of compacted PS nanofibers

PS nanofibers in parallel packaging, which have been compacted under pressure at higher temperature below the glass transition temperature of bulk PS (T_g = 105°C) reveal in the deformation tests that the deformation mechanism is only crazing. The compacted material consists mainly of thicker PS fibers (Fig. 10) show crazes in the thicker fibers of the compacted pattern. The thick compacted fibers, which consists of several individual parallel fibers, show coarse crazes with large nanovoids and irregularly arranged fibrils with thickness from 25 nm up to 200 nm [see Figs. 10(a,b) and 11 (c,d)]. The thick compacted fiber deforms with formation of crazes propagating from one surface to the opposite one, but with interruption of the regular craze fibrillation due to the interfaces between the individual nanofibers. In general, the compacted material deforms such as thicker PS single fibers and, also as bulk material.

The thick fibers show crazes at lower elongations and determine the deformation character. Thinner fibrils with thickness below the thickness limit of about 220–225 nm have no influence on the deformation mechanism.

As mentioned before, the structure of the crazes in compacted PS nanofibers appears coarser than in the single nanofibers, see Figure 12 (and compare with Fig. 7). The reason is partly in the higher stress level in compacted materials and partly also in the limited resolution power of the SEM inspection (Figs. 10 and 11) compared with TEM inspection (Fig. 6). The SEM micrographs reveal only the thicker craze fibrils and not, as in TEM inspection, also all the thinner fibrils.

Thermal analysis (DSC)

The result of determination of glass transition temperature of different materials from DSC analysis is

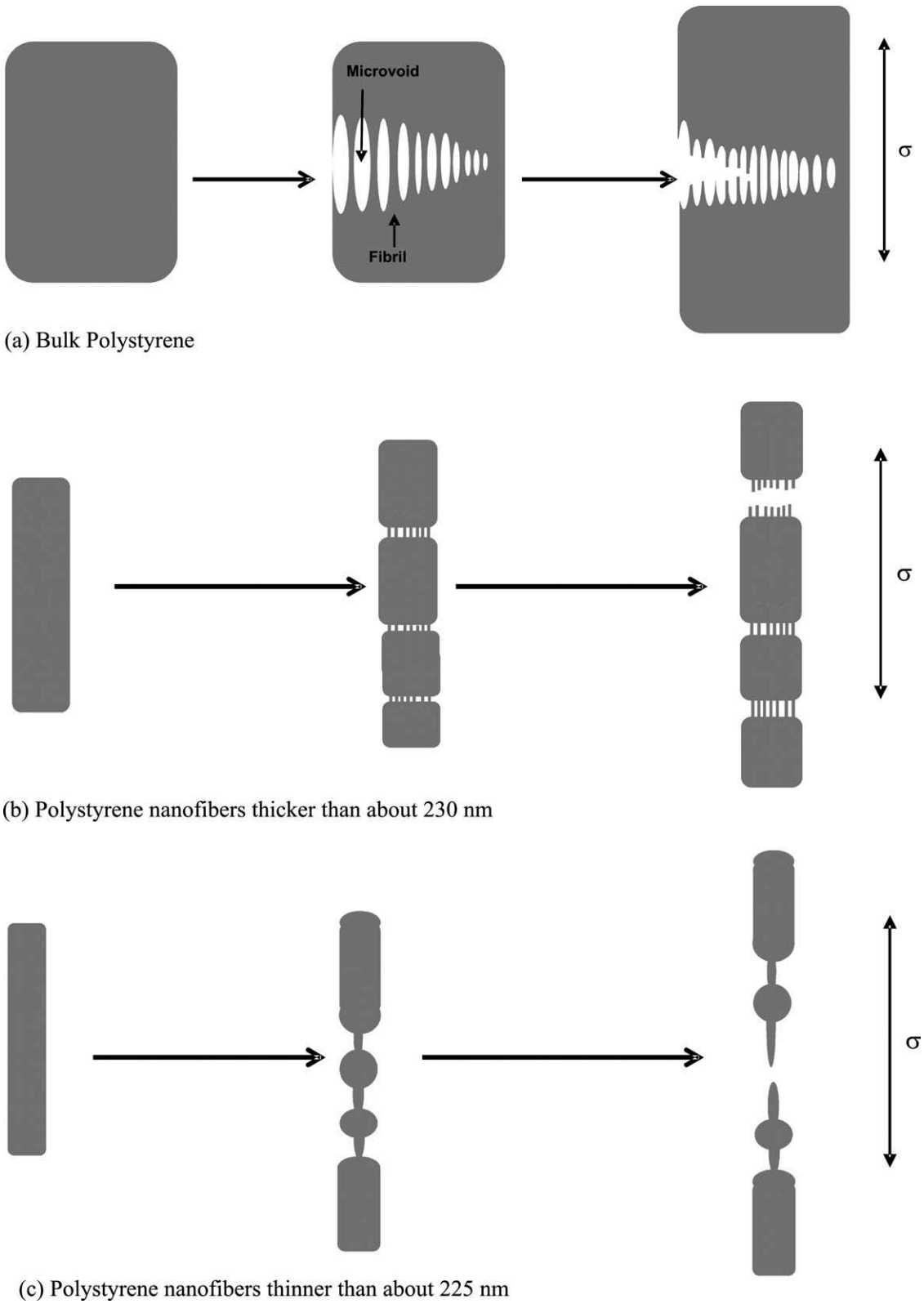

Figure 13 Schematic illustration of micromechanical deformation mechanism of PS in dependence on sample thickness. (a) Bulk polystyrene, (b) PS nanofibers thicker than about 230 nm, (c) PS nanofibers thinner than about 225 nm.

summarized in Table II. Compared to the glass transition temperature of granules of PS (the same as in bulk PS) the fibers show lower values.

DISCUSSION AND CONCLUSIONS

It is well known that bulk PS material deforms with formation of crazes. The features of crazes, stretched

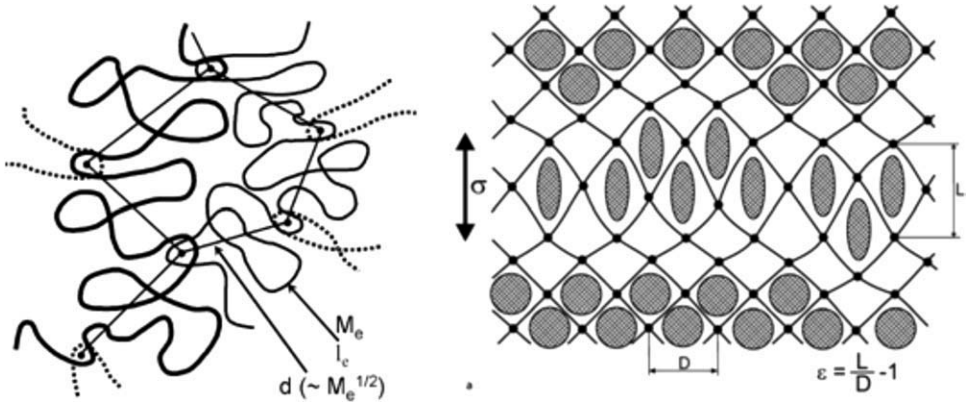

Figure 14 Entanglements and entanglement network in amorphous polymers; M_e, l_e are the molecular weight and the length of the macromolecular segments between entanglements, respectively; d is the distance between entanglements; $\lambda_{max} = \frac{L}{D}$ is the maximum elongation of the network under an applied loading stress (from Ref. [21]).

fibrils between elongated nanovoids, are illustrated in Figure 13(a). From the starting point, e.g., a notch or defect at the surface as a stress concentration point, the craze propagates into the bulk material and usually decreases in thickness. Under additional increase in loading, the craze fibrils rupture and a crack propagates very quickly through the craze. The very fast crack propagation is the typical feature of the brittle fracture of PS.

Hot compacted PS with thick fibers or strands of PS nanofibers reveals the same micromechanical behavior with fibrillated crazes starting from the surface and propagating into the material. Crazes appear also in the thicker nanofibers (thicker than about 225 nm), but with the difference that the crazes penetrate the whole fiber thickness. The average fibril thickness of 10–25 nm and the fibril distances (long period) of 30–60 nm, i.e., diameter of the nanovoids between fibrils of 10–40 nm, correlate very well with the typical features of crazes in bulk PS.[14] The craze length is limited by the fiber thickness, i.e., in the range of a few 100 nm—see Figure 13(b). A very interesting transition in the deformation behavior appears in fibers thinner than $\sim$ 225 nm. Here, the plastic deformation starts with necking of the fiber and thinning up to a thickness of about 50–80 nm. The necking zone is partly localized and partly expanded up to some micrometers, similar to a cold drawing zone. The reduction of the fibril thickness from about 200 nm up to 60–80 nm in the necking zone can be used to estimate a local plastic strain of up to few 100%. This value correlates with the maximum elongation of the entanglement network in PS of about $\lambda_{max} = 400\%$,[22,23] see Figure 14. Such high elongations are also realized in the craze fibrils of bulk PS with the typical fibril thickness of 10–30 nm after stretching. The fibrils are deformed up to some 100% and, therefore, the starting thicknesses of the PS parts before deformation are in the range of 30–60 nm. These results show that plastic yielding in bulk PS starts, if there are material strands between nanovoids thinner than about 60 nm. In such thin strands exists only some entanglement meshes in vertical direction. Therefore, there are no constraints and an easier deformation in length direction is possible.[24]

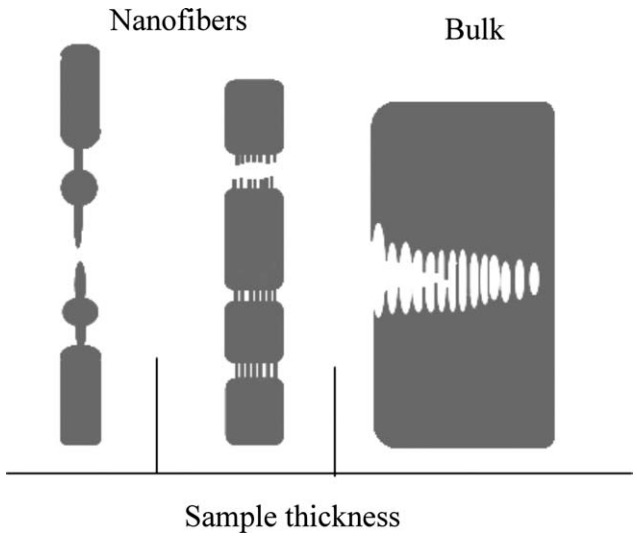

Figure 15 Scheme of change in the deformation mechanism of PS with decreasing sample thickness from bulk material to nanofibers.

Nanofibers, on the other hand, start to necking, if they are thinner than $\sim$ 225 nm. The reason of this larger thickness compared with the thickness of craze fibrils could be found in the free surface of the nanofibers and, therefore, the reduced glass transition temperature T_g (see Table II). This effect could increase molecular mobility and ductility of the material in a modified surface layer around the fibers. If we assume such a modified surface layer with increased mobility in the some thickness than

the PS strands in the crazes, i.e., of about 60 nm, an unmodified core in a thickness range of about (220 – 2 × 60 : 220 – 120) 100 nm remains. It can be assumed that the macromolecules are partly oriented in fiber direction with a change from spherical macromolecular coils as in the bulk to an oriented shape in the fibers. Oriented PS films show a higher crazing stress in orientation direction.[14] In a consequence, with increasing loading the yield stress can be reached earlier than cavitation stress (or crazing stress) and necking occurs. Both effects, the free surface of the nanofibers with increased molecular mobility (and reduced glass transition temperature T_g) and the macromolecular orientation with increased crazing stress, enhance the ductility limit of the nanofibers to the larger values of about 200 nm (compacted to about 60 nm of PS strands in crazing mechanism). The change of deformation mechanism with decreasing specimen thickness of PS from crazing in bulk material to multiple craze formation in thick nanofibers and necking or cold drawing in thinner nanofibers is sketched in Figure 15.

To conclude, the usually typically brittle PS can be modified using electrospinning technique so that a transition from crazing behavior to micronecking and ductile behavior appears. The increased ductility of very thin PS fibers could be used to produce ductile PS networks for different applications for instance networks as flocculants in the treatment of waste water,[25] ion exchanger,[26] for organic electronic applications,[27] for optical application,[28] and scaffolds for biomedical applications.[29]

The authors wish to express their thanks to Dr. Reinhold Godehardt for compaction of the nanofibers and thank Mrs. Stefanie Scholtyssek for her excellent technical assistance during the preparation of miniaturized sample for micromechanical deformation.

References

1. Bhardwaj, N.; Kundu, S. C. Biotechnol Adv 2010, 28, 325.
2. Desai, K.; Kit, K.; Li, J.; Zivanovic, S. Biomacromolecules 2008, 9, 1000.
3. Reneker, D. H.; Chun, I. Nanotechnology 1996, 7, 216.
4. Mirmohseni, A.; Oladegaragoze, A. Synth Met 2000, 114, 105.
5. Kim, G. H. Biomed Mater 2008, 3, 025010.
6. Gibson, P.; Schreuder-Gibson, H.; Rivin, D. Colloids Surf A 2001, 187/188, 469.
7. Huang, Z. M.; Zhang, Y. Z.; Kotaki, M.; Ramakrishna, S. Compos Sci Technol 2003, 63, 2223.
8. Brody, A. L.; Marsh, K. S. Packaging Technology, 2nd ed.; Wiley: New York, 1997.
9. Robertson, G. L. Food Packaging, Principles and Practices; Marcel Dekker Inc.: New York, 1992.
10. Kim, G.-T.; Hwang, Y.-J.; Ahn, Y.-C.; Shin, H.-S.; Lee, J.-K.; Sung, C.-M. Korean J Chem Eng 2005, 22, 147.
11. Shin, C. Y.; Chase, G. G. Polym Bull 2005, 55, 209.
12. Moon, S.; Choi, J.; Farris, R. J. Fibers Polym 2008, 9, 276.
13. Kausch, H. H. Crazing in Polymers, Advances in Polymer Science; Springer: Berlin, Heidelberg, New York, 1992; Vol.91/92.
14. Michler, G. H. Kunststoff-Mikromechanik: Morphologie, Deformations- und Bruchmechanismen; Carl Hanser: München, 1992.
15. Tan, E. P. S.; Lim, C. T. Compos Sci and Technol 2006, 66, 1102.
16. Carlisle, C. R.; Coulais, C.; Namboothiry, M.; Carroll, D. L.; Hantgan, R. R.; Guthold, M. Biomaterials 2009, 30, 1205.
17. Henkee, C. S.; Kramer, E. J. J Mater Sci 1986, 21, 1398.
18. Zhou, C.; Bao, X. Y.; Tan, Z. Y.; Sun, S. L.; Ao, Y. H.; Yang, H. D.; Zhang, H. X. J Polym Sci Part B: Polym Phys 2006, 44, 687.
19. Xin, Y.; Huang, Z. H.; Li, W. W.; Jiang, Z. J.; Tong, Y. B.; Wang, C. Eur Polym J 2008, 44, 1040.
20. Teo, W. E.; Ramakrishna, S. Nanotechnology 2005, 16, 1878.
21. Michler GH. Electron Microscopy of Polymers. Berlin: Springer; 2008.
22. Donald, A. M.; Kramer, E. J. Polymer 1982, 23, 461.
23. Kramer, E. J. Polym Eng and Sci 1984, 24, 761.
24. Michler, G. H.; Kausch, H. H.; Adhikari, R. J Macromol Sci B 2006, 45, 727.
25. Sulkowski, W. W.; Wolinska, A.; Szolysik, B.; Bajdur, W. M.; Sulkowska, A. Polym Degrad and Stabil 2005, 90, 272.
26. An, H.; Shin, C.; Chase, G. G. J Membr Sci 2006, 283, 84.
27. Prime, D.; Paul, S. Vacuum 2010, 84, 1240.
28. Kuznetsov, V.; Sheremet'ev, S. J Anal Chem 2007, 62, 270.
29. Byun, J.-W.; Kim, J.-U.; Chung, W.-J.; Lee, Y.-S. Macromol Biosci 2004, 4, 512.